articles

molecular pharmaceutics

Anticancer Efficacy of Squalenoyl Gemcitabine Nanomedicine on 60 Human Tumor Cell Panel and on Experimental Tumor

L. Harivardhan Reddy,[†,‡] Jack-Michel Renoir,[†] Veronique Marsaud,[†] Sinda Lepetre-Mouelhi,[§] Didier Desmaële,[§] and Patrick Couvreur*[,†]

Université Paris-Sud XI, Faculté de Pharmacie, UMR CNRS 8612, IFR 141, 92296 Châtenay-Malabry Cedex, France, and Université Paris XI, Faculté de Pharmacie, UMR CNRS 8076 Biocis, 92296 Châtenay-Malabry Cedex, France

Received April 6, 2009; Revised Manuscript Received July 23, 2009; Accepted July 27, 2009

Abstract: Gemcitabine (2′,2′-difluorodeoxyribofuranosylcytosine) is an anticancer nucleoside analogue active against a wide variety of solid tumors. However, following intravenous administration, this drug is rapidly inactivated by enzymatic deamination and displays a short biological half-life necessitating the administration of high doses leading also to unwanted side effects. To overcome these drawbacks and to improve the therapeutic index of gemcitabine, we have recently developed the concept of *squalenoylation* which consisted in the bioconjugation of gemcitabine with squalene, a natural lipid. In our preliminary studies, we have shown that this bioconjugate (SQgem) self-organized in water as nanoassemblies with considerable resistance to deamination and significantly higher anticancer activity compared with gemcitabine in an intravenously grafted tumor model in mice. To further establish the candidature of this nanomedicine for clinical trials, in this communication we have tested the preclinical efficacy of squalenoyl gemcitabine nanomedicine on several human tumor cell lines and on the subcutaneously grafted experimental L1210 murine tumor in mice. SQgem nanomedicine displayed an efficient cytotoxicity against a variety of human tumor cell lines in the 60 human tumor cell panel. In vivo, following intravenous administration, SQgem nanomedicine displayed a superior anticancer activity against subcutaneous L1210 tumor, comparatively to gemcitabine. The molecular mechanism behind the anticancer efficacy of SQgem has been investigated by flow cytometry analysis and protein expression profiling of L1210wt cells treated in vitro with the squalenoyl gemcitabine bioconjugate. It was found that this nanomedicine arrested the cell cycle in G2/M, characterized by an increased cyclin A and cyclin E expression, and activation of caspase-3 and the cleavage of poly(ADP-ribose) polymerase with an increase of cytochrome C level. Taken together, these results suggest that the cell kill by this nanomedicine occurred through mitochondrial apoptotic triggered pathway, similarly to that of gemcitabine free.

Keywords: Gemcitabine; squalenoylation; squalenoyl gemcitabine; nanomedicine; apoptosis; cancer; preclinical

Introduction

Gemcitabine is a nucleoside analogue which has demonstrated significant anticancer activity against a wide variety of solid tumors, including colon, lung, pancreatic, breast, bladder and ovarian cancers.[1−3] However, treatment by this drug is limited by rapid deamination into the inactive uracil derivative, hence resulting in a short half-life after intravenous administration.[4,5] Therefore, high doses are required for therapeutic activity which contributes to severe side effects of gemcitabine.[6] To overcome these inconveniences and to improve the thera-

* Corresponding author. Mailing address: Université Paris-Sud XI, UMR CNRS 8612, 5 rue J-B Clément, 92296 Châtenay-Malabry Cedex, France. Phone: +33 1 46 83 53 96. Fax: + 33 1 46 61 93 34. E-mail: patrick.couvreur@u-psud.fr.

† Université Paris-Sud XI, UMR CNRS 8612.

‡ Present address: Sanofi-aventis, 13 Quai Jules Guesdes, 94403, Vitry-sur-Seine, France.

§ Université Paris XI, UMR CNRS 8076 Biocis.

(1) Lund, B.; Hansen, O. P.; Theilade, K.; Hansen, M.; Neijt, J. P. Phase II study of gemcitabine (2′,2′-difluorodeoxycytidine) in previously treated ovarian cancer patients. *J. Natl. Cancer Inst.* **1994**, *86*, 1530–1533.

10.1021/mp900099e CCC: $40.75
Published on Web 07/27/2009

peutic index of gemcitabine, we recently developed the concept of *squalenoylation* which consisted of the bioconjugation of gemcitabine with squalene, a natural lipid, precursor of the cholesterol's biosynthesis.[7] It was observed that the squalenoyl gemcitabine bioconjugate spontaneously self-organized in water as nanoassemblies displaying hexagonal supramolecular nanostructures of 130 nm size.[8] SQgem nanoassemblies are unique and possess important characteristic properties compared to other gemcitabine conjugates, such as (i) self-association into nanoassemblies in water without the aid of surfactant unlike that of other fatty acid-gemcitabine conjugates, i.e. 4-(*N*)-valeroyl-, 4-(*N*)-heptanoyl-, 4-(*N*)-lauroyl- and 4-(*N*)-stearoyl-gemcitabine, which are highly lipophilic and form large aggregates in water[9] restricting the possibility of direct iv administration; (ii) demonstrated resistance to deamination both in vitro in the presence of deaminase enzyme and in vivo following iv injection;[10,11] and (iii) improved pharmacokinetics and controlled drug exposure after iv administration.[11]

The preliminary investigations concerning the anticancer efficacy of the squalenoylated gemcitabine (SQgem) were performed in mice experimental leukemia obtained by direct injection of the leukemia cells into the blood; in these conditions, we showed the improved anticancer activity of SQgem nanoassemblies over the parent drug gemcitabine,[12] but the related molecular mechanisms and cell death pathway remained unknown. Toxicological studies on mice have revealed that the toxicity profile of SQgem nanoassemblies was similar to that of gemcitabine, no additional toxicities being encountered with this nanomedicine.[13] Inspired by these encouraging preliminary data and to further support the candidature of SQgem nanoassemblies to clinical trials, we have extended our investigations to the in vitro treatment of 60 human tumor cell panel under National Cancer Institute's drug screening program. The in vivo determination of the anticancer activity of SQgem nanoassemblies was performed in subcutaneously grafted L1210 tumor model, since in this model the tumor endothelium represents an additional barrier to be overcome by SQgem before exerting its pharmacological activity. The anticancer efficacy was further assessed using histological and immunohistochemistry techniques, and the molecular mechanism behind the anticancer activity of SQgem has been additionally investigated.

Materials and Methods

Chemicals. Gemcitabine hydrochloride was purchased from Sequoia Research Products Ltd. (U.K.). Squalene and dextrose were purchased from Sigma-Aldrich Chemical Co., France. Matrigel Matrix Growth Factor Reduced was purchased from Becton Dickinson biosciences (USA).

Synthesis of 4-(*N*)-Trisnorsqualenoyl Gemcitabine. 4-(*N*)-Trisnorsqualenoyl gemcitabine (SQgem) was synthesized as reported earlier.[14] Briefly, to a stirred solution of 1,1′,2-*tris*norsqualenoic acid (0.5 g, 1.2 mM) in anhydrous THF (3 mL) was added dropwise triethylamine (0.150 g, 1.5 mM). The mixture was cooled to −15 °C, and a solution of ethyl chloroformate (0.135 g, 1.2 mM) in anhydrous THF (3 mL) was added dropwise. The mixture was stirred at 0 °C for 15 min, and a solution of gemcitabine hydrochloride (dFdC HCl) (0.37 g, 1.2 mmol) with triethylamine (0.24 g, 2.4 mM) in anhydrous DMF (5 mL) was added dropwise to the reaction at the same temperature. The reaction was stirred 72 h at room temperature, and the reaction mixture was then concentrated *in vacuo*. Aqueous sodium hydrogen carbonate was added, and the mixture was extracted with ethyl acetate (3 × 50 mL). The combined extracts were washed with water, dried on $MgSO_4$, and evaporated. The crude product was purified by chromatography on silica gel and eluted with CH_2Cl_2/MeOH/Et_3N 100:2:1 then with CH_2Cl_2/MeOH/Et_3N 100:5:1 to give pure 4-*N*-squalenoyl-gemcitabine (0.46 g, 57%) as an amorphous white solid: $[\alpha]_D = 3.1$ ($c = 0.95$, CH_2Cl_2); IR (neat, cm^{-1}) ν 3500−3150, 2950, 2921, 2856, 1709, 1656, 1635, 1557, 1490, 1435, 1384, 1319, 1275, 1197, 1130, 1071, 814; ^1H NMR (300 MHz, $CDCl_3$) δ 9.15 (s large, 1H, NHCO), 8.16 (d, 1H, $J = 7.5$ Hz, H6), 7.47 (d, 1H, $J =$ 7.5 Hz, H5), 6.18 (t, 1H, $J = 7.0$ Hz, H1′), 5.22−5.15 (m,

(2) Anderson, H.; Lund, B.; Bach, F.; Thatcher, N.; Walling, J.; Hansen, H. H. Single agent activity of weekly gemcitabine in advanced non-small-cell lung cancer: a phase II study. *J. Clin. Oncol.* **1994**, *12*, 1821–1826.

(3) Catimel, G.; Vermorken, J. B.; Clavel, M.; et al. A phase II study of gemcitabine (LY188011) in patients with advanced squamous carcinoma of the head and neck. *Ann. Oncol.* **1994**, *5*, 543–547.

(4) Abbruzzese, J. L.; Grunewald, R.; Weeks, E. A.; et al. A phase I clinical, plasma, and cellular pharmacology study of gemcitabine. *J. Clin. Oncol.* **1991**, *3*, 491–498.

(5) Reid, J. M.; Qu, W.; Safgren, S. L.; et al. Phase I trial and pharmacokinetics of gemcitabine in children with advanced solid tumors. *J. Clin. Oncol.* **2004**, *22*, 2445–2451.

(6) Reddy, L. H.; Couvreur, P. Novel approaches to deliver gemcitabine to cancers. *Curr. Pharm. Des.* **2008**, *14*, 1124–1137.

(7) Couvreur, P.; Stella, B.; Cattel, L.; et al. Nanoparticules de derives de la gemcitabine. *French Patent*, WO/2006/090029, 2006.

(8) Couvreur, P.; Reddy, L. H.; Mangenot, S.; et al. Discovery of new hexagonal supramolecular nanostructures formed by squalenoylation of an anticancer nucleoside analogue. *Small* **2008**, *4*, 247–253.

(9) Myhren, F.; Borretzen, B.; Dalen, A.; et al. Gemcitabine derivatives. Eur Patent EP0986570, 2000.

(10) Reddy, L. H.; Ferreira, H.; Dubernet, C.; et al. Squalenoyl nanomedicine of gemcitabine is more potent after oral administration in leukemia-bearing rats: study of mechanisms. *Anticancer Drugs* **2008**, *19*, 999–1006.

(11) Reddy, L. H.; Khoury, H.; Paci, A.; et al. Squalenoylation favourably modifies the in vivo pharmacokinetics and biodistribution of gemcitabine in mice. *Drug Metab. Dispos.* **2008**, *36*, 1570–1577.

(12) Reddy, L. H.; Dubernet, C.; Mouelhi, S. L.; et al. A new nanomedicine of gemcitabine displays enhanced anticancer activity in sensitive and resistant leukemia types. *J. Controlled Release* **2007**, *124*, 20–27.

(13) Reddy, L. H.; Marque, P. E.; Dubernet, C.; et al. Preclinical toxicology (sub-acute and acute) and efficacy of a new squalenoyl gemcitabine anticancer nanomedicine. *J. Pharmacol. Exp. Ther.* **2008**, *325*, 484–490.

(14) Couvreur, P.; Stella, B.; Reddy, L. H.; et al. Squalenoyl nanomedicines as potential therapeutics. *Nano Lett.* **2006**, *6*, 2544–2548.

5H, H*vinyl*), 4.49 (m, 1H, H3′), 4.86−4.09 (m, 3H, H4′, 2H5′), 2.55 (m, 2H, $COCH_2CH_2$), 2.38−2.28 (m, 2H, $COCH_2CH_2$), 2.13−1.91 (m, 16H, CH_2), 1.69−1.55 (m, 18H, C=C(CH_3)); ^{13}C NMR (100 MHz, $CDCl_3$) δ 173.7 (CONH), 163.0 (CO), 155.8 (C), 145.4 (CH), 135.1 (C), 134.9 (2 C), 132.7 (C), 131.1 (C), 125.7 (CH), 124.4 (CH), 124.3 (CH), 124.2 (2 CH), 122.3 (t, $J_{CF} = 260$ Hz, CF_2), 97.7 (CH), 85.8 (m, CH), 81.6 (CH), 69.2 (t, $J = 21$ Hz, CH), 59.7 (CH_2), 39.7 (2 CH_2), 39.5 (CH_2), 36.5 (CH_2), 34.3 (CH_2), 29.6 (CH_2), 28.3 (CH_2), 26.8 (CH_2), 26.7 (CH_2), 26.6 (CH_2), 25.6 (CH_3), 17.6 (CH_3), 16.0 (2 CH_3), 15.9 (CH_3), 15.8 (CH_3); MS (-ESI) $m/z = 644$ ([M − H]$^-$, 100%). Anal. Calcd for $C_{36}H_{53}F_2N_3O_5$: C, 66.95, H, 8.27, N, 6.51. Found: C, 66.76, H, 8.40, N, 6.39.

Formulation and Characterization of Squalenoyl Gemcitabine Nanoassemblies. 4-(*N*)-Tris-nor-squalenoyl-gemcitabine nanoassemblies (SQgem) were prepared by nanoprecipitation. Briefly, SQgem (4 mg) was dissolved in ethanol (0.4 mL) and added dropwise under stirring (500 rpm) into 1 mL of 5% aqueous dextrose solution. Precipitation of the SQgem nanoassemblies occurred spontaneously. Ethanol was completely evaporated using a Rotavapor at 37 °C to obtain an aqueous suspension of pure SQgem nanoassemblies. Finally, the nanoassemblies' dispersion was adjusted to 1 mL with water for injection.

SQgem nanoassemblies suspension has been analyzed using high performance liquid chromatography−mass spectrometry (LC−MS) technique reported previously,[15] to verify the concentration of SQgem in the final product.

The mean particle size and polydispersity index were determined at 20 °C by quasi-elastic light scattering (QELS) with a nanosizer (Coulter N4MD, Coulter Electronics, Inc., Hialeah, FL). The selected angle was 90°, and the measurement was made after dilution of the nanoassembly suspension in Milli-Q water. The zeta potential was determined using zetasizer (Zetasizer 4, Malvern Instruments Ltd., U.K.) after dilution with 5% aqueous dextrose.

The morphology of the SQgem nanoassemblies was observed by cryo-transmission electron microscopy after vitrification using a JEOL FEG-2010 electron microscope. Micrographs were recorded at 200 kV under low-dose conditions at a magnification of 40,000 on SO-163 Kodak films. Micrographs were digitized using a film scanner (Super coolscan 8000 ED, Nikon), and analysis was made using the ImageJ software.

Cell Lines. The in vitro anticancer activity studies were performed on human cancer cells under the National Cancer Institute's (NCI) DTP human tumor cell line screen, using NCI's 60 human cancer cell line panel. Briefly, the cells were grown in RPMI 1640 medium containing 5% fetal bovine serum and 2 mM L-glutamine. Depending on the doubling time of the cell lines, about 5,000 to 40,000 cells/well were preincubated for 24 h. After 24 h, the cells were incubated with various concentrations of SQgem nanoassemblies and incubated for 48 h at 37 °C, 5% CO_2. The cytotoxicity test was performed using Sulforhodamine B assay. The dose response parameters such as growth inhibition 50% (GI50), total growth inhibition (TGI) and lethal concentration 50% (LC50) were calculated. GI50 is the concentration of drug required to decrease the cell growth to 50%, compared with that of the untreated cell number. TGI is the concentration of drug required to decrease the cell growth to 100%, compared with that of the untreated cell number, during drug incubation. LC50 is the concentration of drug required to decrease the cell growth by 50% of the initial cell number prior to the drug incubation.

L1210 wt (a murine lymphoid leukemia) cell line was cultured in RPMI 1640 supplemented with 10% fetal calf serum, 50 U mL^{-1} penicillin, 50 μg mL^{-1} streptomycin and 2 mM L-glutamine. The anticancer activity of gemcitabine, pure squalene nanoparticles and SQgem nanoassemblies against this cell line was determined using the 3-[4,5-dimethylthiazol-2-yl]-3,5-diphenyl tetrazolium bromide (MTT) test, measuring mitochondrial dehydrogenase activity. L1210 wt cells in exponential growth phase were seeded into 96-well plates and were preincubated for 24 h at 37 °C in a humidified atmosphere of 5% CO_2 in air. Different dilutions of gemcitabine and of SQgem nanoassemblies were added to the cells in the culture medium. Each dilution was tested in triplicate. After 72 h at 37 °C, 200 μL of MTT solution in cell culture medium (0.5 mg/mL) was added to each well. After incubation for 2.5 h at 37 °C, the culture medium was removed and the resultant formazan crystals were dissolved in 200 μL of extraction solution (1:1 ratio of sodium dodecyl sulfate 20% solution and dimethyl formamide). The absorbance of converted dye, which is proportional to the number of viable cells, was measured at 570 nm using a microplate reader (Metertech Σ 960, Fisher Bioblock, Illkirch, France). The percentage of surviving cells was calculated as the absorbance ratio of treated to untreated cells.

Cell Cycle Analysis. L1210 wt cells were incubated with gemcitabine (5 nM) or SQgem nanoassemblies (5 nM) for 72 h in 96 well plates. At 72 h postincubation, the untreated and treated cells were analyzed for cell cycle by flow-cytometric measurements of cellular DNA content using the DNA-intercalating fluorochrome, propidium iodide (PI). Briefly, the cells were washed once with 2 mL of pH 7.4 phosphate buffered saline (PBS). About 1×10^6 cells were fixed overnight in 70% ethanol. The cells were centrifuged to remove ethanol, washed with PBS and treated with extraction buffer (a mixture of 192 parts of 0.2 M disodium hydrogen phosphate and 8 parts of 0.1 M citric acid). After that, the cells were washed with 2 mL of PBS and treated with ribonuclease-A (200 μg/mL) for 30 min at 37 °C. Then, the cells were stained with PI (50 μg/mL) in PBS. Measurements were made with a laser-based (488 nm) flow cytometer (FACS Calibur; Beckton and Dickenson, USA) and data acquired using the Cell Quest software (Beckton and

(15) Khoury, H.; Deroussent, A.; Reddy, L. H.; et al. Simultaneous determination of gemcitabine and gemcitabine-squalene by liquid chromatography-tandem mass spectrometry in human plasma. *J. Chromatogr., B: Anal. Technol. Biomed. Life Sci.* **2007**, *858*, 71–78.

Dickenson, USA). Off-line gating was performed using appropriate windows created by analysis of light scattering from untreated cells.

Protein Expression and Cleavage Profiling in L1210 Wt Leukemia Cells after Incubation with Gemcitabine or Squalenoyl-Gemcitabine Nanoassemblies. To the confluent suspension of L1210 wt murine leukemia cells was added gemcitabine (10 nM and 20 nM) or SQgem nanoassemblies (10 nM and 20 nM equiv of gemcitabine) and incubated for 20 h at 37 °C. Then, the cells were centrifuged at 2000 rpm, 4 °C for 10 min. The cell pellet was washed with 10 mL of cold phosphate buffered saline (PBS) and again centrifuged. The untreated cells were also washed similarly. To the cell pellet was added 100 μL lysis buffer containing complete protease inhibitors. This cell suspension was then placed on ice for 30 min. The cell suspension was then diluted with water, and protein estimation was performed using Bradford assay at 595 nm.

Acrylamide denatured (SDS) gel 15% (for poly(ADP-ribose) polymerase (PARP) and cytochrome *c* (Cyt *c*)) and 10% (for caspase-3, cyclin A, cyclin E and hsp70) was cast. 50 μg/protein/well equivalent of the samples was loaded onto the gel, and migration was carried out for 60 min under 40 mA/gel. The proteins were then transferred onto the immobilized PVDF membrane, and migration was carried out for 75 min under 50 mA/membrane. Later, the membranes were washed and incubated with 10% dry nonfat milk for 1 h at room temperature. After that, the membranes were washed thrice for 10 min with PBS containing 1% tween 20 (PBST). The membranes were then incubated overnight at 4 °C with 1 μg/mL of rabbit antibodies against activated caspase-3 (E8), cyclin A (BF 683), cyclin E (M 20), cytochrome C (7H8), hsp70 (W7) and PARP (F2) all from Santa Cruz biotechnology Inc. (Santa Cruz, CA). The membranes were then washed thrice for 10 min with PBST, and then incubated with horse radish peroxidase (HRP)-labeled mouse anti-rabbit antibody for 2 h at room temperature. Then, the membranes were washed thrice for 10 min with PBST, and revealed by Luminol (Santa Cruz, CA) using autoradiography.

In Vivo Anticancer Activity Studies. The animal experiments were carried out according to the principles of laboratory animal care and legislation in force in France. DBA/2 mice (4−5 weeks old) weighing about 13−16 g were used for the study. The mice were provided with standard mouse food and water ad libitum. The L1210 wt (a murine lymphocytic leukemia) cells were maintained in vitro, and were mixed prior to injection, with 30% Matrigel (matrix growth factor reduced) in cell culture medium kept on ice. The cell suspension equivalent to 1×10^6 cells was injected subcutaneously into mice toward the upper portion of the right flank, to develop a solid tumor model.

After the mice developed palpable tumors (of an average volume of 240 mm^3), they were randomly divided into 4 groups of 7−8 each, i.e. untreated, treated with pure squalene nanoparticles 100 mg/kg, treated with gemcitabine 100 mg/kg (MTD), and treated with SQgem nanoassemblies 20 mg/kg equivalent to gemcitabine (MTD). On days 0, 4, 8 and 13, all groups of mice except the untreated group received the treatment by intravenous route. The mice were monitored regularly for changes in tumor size.

Preparation of Tumors for Histology and Immunohistochemistry Evaluations. Following the completion of treatment schedule using gemcitabine or SQgem nanoassemblies, one mouse from each group (i.e., untreated and treated) was sacrificed and the tumors were isolated. The tumors were fixed overnight in Finefix at room temperature. Next day, the tumors were washed by placing in ethanol and toluene, and fixed in paraffin. For immunohistochemical studies, 3 μm sized paraffin embedded tumor sections were cut using a microtome blade, fixed on the glass slide for overnight at 56 °C.

Hematoxylin−Eosin−Saffron (HES) Staining. The tumor sections were analyzed by optical microscopy using the HES staining technique. Briefly, paraffin embedded tumor sections were deparaffinated by dipping in toluene and ethanol, and washed with purified water. Then, the tumor sections were stained using hematoxylin, eosin and saffron by successive washings in water or ethanol and finally with toluene. Subsequently, the sections were mounted for observation under a microscope.

Proliferation Index Measurement in Tumor Cells. Cell proliferation was confirmed using the Ki-67 labeling test. Ki-67 is a nuclear antigen expressed in proliferating cells in the late G_1, S, G_2, and M phases but is absent in resting cells (G_0).[16] Purified mouse anti-human KI-67 antibody (BD Pharmingen) was used for the demonstration of the Ki-67 antigen. Paraffin embedded tumor sections prepared from the untreated or treated tumors collected from mice, and human tonsil tissue section (a positive control for KI-67 antigen) were deparaffinated by washing the sections with toluene, ethanol and purified water. Demasking of epitope was performed in citrate buffer at 85−90 °C. Then, the hydrophobic markings were performed around the tumor sections. The endogenous peroxidases were blocked by incubating the tissue sections using 0.3% H_2O_2 solution. To prevent the nonselective binding of antibody, the tissue sections were incubated with horse normal serum (Vectastain). Then, the tissue sections were incubated with anti-human KI-67 antibody for 1 h, followed by incubation with antimouse IgG biotinylated antibody. To ensure specific staining of the KI-67 positive cells, the tissue sections were also treated separately with either first antibody or second antibody. The tissue sections were washed with PBS and incubated with avidin−biotin mixture for 30 min. Later, the tissue sections were incubated with diaminobenzidene in the dark for 10 min, washed with PBS, colored with hematoxylin and mounted for observation under a microscope. The labeled cells were counted under 40× magnification, of three different slides of each tumor sample. The significance of

(16) Scholzen, T.; Gerdes, J. The Ki-67 protein: from the known and the unknown. *J. Cell Physiol.* **2000**, *182*, 311–322.

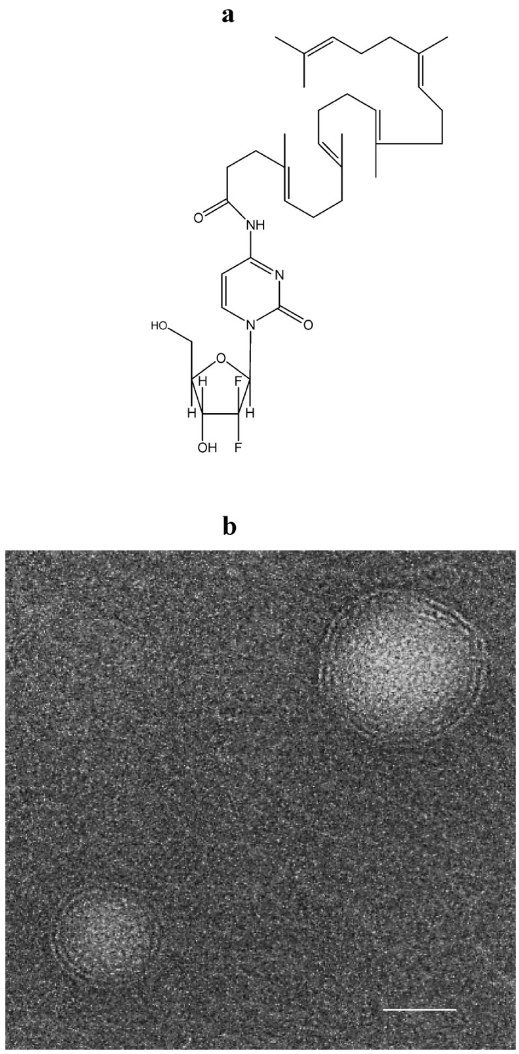

Figure 1. (a) Chemical structure of 4-(*N*)-Trisnorsqualenoyl gemcitabine. (b) Morphological appearance of SQgem nanoassemblies under cryo-transmission electron microscope. Bar: 45 nm.

difference between treatment groups was determined by the two-tailed Student's *t* test.

Results

Characterization of Nanoassemblies. The mean diameter of the obtained SQgem nanoassemblies was 129 ± 8 nm, with a unimodal size distribution (0.1), as measured by quasi-elastic light scattering. Under cryo-transmission electron microscopy, SQgem nanoassemblies appeared as round shaped and surrounded by an external shell (Figure 1).

In Vitro Anticancer Activity of SQgem Nanoassemblies under NCI Screening Program. In vitro, SQgem nanoassemblies were found to be impressively active on variety of cancers studied using NCI's 60 human cancer cell line panel. Three dose−response parameters were calculated such as GI50, TGI and LC50 (Table 1). Noteworthy, in a variety of cell lines studied under each type of cancer, the SQgem displayed GI50 at nanomolar concentrations.

Table 1. In Vitro Anticancer Activity of Squalenoyl Gemcitabine (SQgem) Nanoassemblies on a 60 Human Tumor Cell Line Panel Performed under National Cancer Institute's Developmental Therapeutics Program[a]

	response parameters		
cell line	GI50 (μM)	TGI (μM)	LC50 (μM)
	Leukemia		
CCRF-CEM	0.109	1.1	>100
HL60 (TB)	0.185	1.45	36
K-562	2.31	78	>100
MOLT-4	0.13	3.41	76.3
RPMI-8226	0.173	0.771	99.2
	NSCLC		
A549/ATCC	0.0555		>100
EKVX	0.276	18.9	50
HOP-62	0.0293	0.299	24.5
HOP-92	0.218	6.83	40.2
NCI-H226	0.73	18.2	50.8
NCI-H23	0.0323	6.04	40.6
NCI-H322M	0.37	15	40.9
NCI-H460	0.0349	1.13	3.52
NCI-H522	0.0528	1.91	5.32
	Colon Cancer		
COLO 205	0.0982	12.6	54.4
HCC-2998	0.069	18.1	45.8
HCT-116	0.0151	0.0576	2.57
HCT-15	0.856	22.6	66.3
HT-29	0.576	29.4	>100
KM12	0.375	16.9	45.6
SW-620	0.867	23.5	65.7
	CNS Cancer		
SF-268	0.114	0.928	29.7
SF-295	0.0554	0.403	21.4
SF-539	0.0142	0.495	19.5
SNB-19	0.0168	10.1	37.3
SNB-75	0.788	19.5	80.9
U251	0.0993	15.6	43.9
	Melanoma		
LOX IMVI	0.374	14.2	50.8
MALME-3M	0.438	6.7	30
M14	0.0283	0.135	1.12
SK-MEL-2	0.0183	1.28	5.03
SK-MEL-28	11.9	25.2	53.6
SK-MEL-5	0.0851	1.58	3.98
UACC-257	0.0988	2.7	7.79
UACC-62	0.252	14.7	42.2
	Ovarian Cancer		
IGROV1	0.115	5.15	53.8
OVCAR-3	<0.01	1.1	22.8
OVCAR-4	1.39	3.6	9.34
OVCAR-5	0.0955	20.8	49.5
OVCAR-8	0.022		>100
SK-OV-3	0.0574	15.1	41.1
	Renal Cancer		
786−0	<0.01	<0.01	0.0101
A498	0.0741	19.4	46.3
ACHN	0.0323	10.4	33.3
CAKI-1	0.0583	12.1	34.8
RXF-393	1.09	7.15	54.3
SN12C	0.347	12.9	41.9
TK10	3.23	19.1	46.3
UO-31	0.0432	10.5	40.4
	Prostate Cancer		
PC-3	4.47	22.1	54.8
DU-145	0.049	2.4	29.5
	Breast Cancer		
MCF7	<0.01	1.27	4.41
NCI/ADR-RES	0.0578	11.9	41.7
MDA-MB-231/ATCC	12.3	26.6	57.4
HS578T	14.9	39.5	>100
MDA-MB-435	0.349	15.8	42
BT-549	0.295	6.05	29.7
T-47D	0.0621	9.87	50.9
MDA-MB-468	0.531	52.4	>100

[a] The cells were incubated with various concentrations of SQgem nanoassemblies for 48 h. GI50 = growth inhibition 50%, TGI = total growth inhibition, LC50 = lethal concentration 50%.

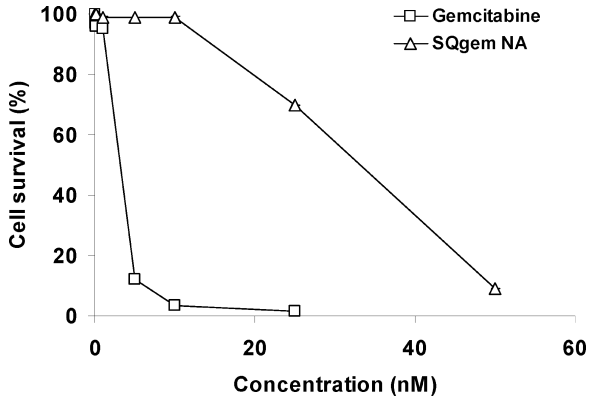

Figure 2. In vitro cytotoxicity curve of SQgem nanoassemblies (SQgem NA) versus gemcitabine on L1210 wt murine leukemia cell line. Squalene nanoparticle formulation at dilutions corresponding to that of SQgem nanoassemblies was used as a placebo control. The values are the mean ± SD of three determinations. The SD is not visible on the curves due to small variation intensities. Squalene nanoparticles did not show any toxicity at the dilutions tested.

Table 2. Percentage of L1210 Leukemia Cells in Various Phases of the Cell Cycle, Following in Vitro Incubation with Gemcitabine (5 nM) or Squalenoyl Gemcitabine Nanoassemblies (SQgem) (5 nM) for 72 h[a]

treatment	G0/G1 phase	S phase	G2/M phase	sub-G1
untreated	77.65	19.72	2.63	3.86
gemcitabine	27.17	70.67	2.16	65.96
SQgem nanoassemblies	54.78	3.19	42.03	9.50

[a] A clear G2/M accumulation of cells after SQgem nanoassembly treatment could be noticed with a small population of cells in sub-G1, considerably lower than after free gemcitabine treatment.

When incubated for 72 h with L1210 wt cell line (a murine lymphoid leukemia), the SQgem nanoassemblies exhibited a lower cytotoxicity, as compared with free gemcitabine (Figure 2).

Cell Cycle Analysis and Protein Expression Profiling. Gemcitabine treatment of L1210 wt cells for 72 h led to a considerable accumulation of cells in the S-phase (65.96%), and a reduced G0/G1 phase (27.17%) compared with untreated cells (77.65%) (Table 2). On the contrary, SQgem nanoassembly treatment led to a greater accumulation of cells in G2/M phase (G2/M arrest) and a reduced percentage of cells in the S-phase. Additionally, the gemcitabine-treatment led to a considerably greater apoptosis induction in L1210 wt cells compared with SQgem nanoassemblies.

Exposure of L1210 wt cells to SQgem nanoassemblies at concentrations equivalent to its parent drug gemcitabine (i.e., 10 nM and 20 nM equivalent) led to the cell cycle arrest characterized by an increased cyclin A and cyclin E expression (Figure 3). Simultaneously, caspase-3 was also found activated at the highest gemcitabine and SQgem concentrations, as revealed by detection of faint bands at 20 and 17 kDa. Concomitantly, SQgem nanoassemblies treatment led to the enhanced cleavage of PARP compared with gemcitabine free. Cytochrome "C" level was also found increased in case of SQgem nanoassembly treated cells, similarly to that of the gemcitabine-treated cells.

Anticancer Activity of SQgem Nanoassemblies against L1210 Tumor. The anticancer activity of SQgem nanoassemblies was studied against L1210 subcutaneously grafted tumors in mice, following intravenous injections of the MTDs of gemcitabine or SQgem nanoassemblies on days 0, 4, 8, and 13. After the development of palpable tumors (of about 240 mm^3), the untreated tumor bearing mice died between days 10 and 20. Gemcitabine treatment led to a considerable arrest of tumor progression, whereas the SQgem nanoassembly treated group exhibited a still significantly higher anticancer activity in comparison to gemcitabine free ($P < 0.001$) (Figure 4). On the contrary, squalene nanoparticles injected at a dose of 100 mg/kg (similar injection schedule) did not display any anticancer activity against tumors in mice.

Following the completion of the treatment, one mouse from each group was sacrificed and the tumors were isolated and processed for histological observation using the HES staining technique. The tumor sections of untreated and gemcitabine-treated mice showed a highly dense cancerous tissue. On the contrary, SQgem treatment caused a considerable lowering of tumor cell population, dispersed among large tracks of fibrotic tissue (Figure 5).

The tumor sections were further investigated by immunohistochemistry, using the KI-67 antigen cell proliferation test. The tumor sections revealed a large population of KI-67 positive proliferating tumor cells which were stained brown. The tumor sections of the gemcitabine-treated mouse showed a decreased population of proliferating cells as compared to the tumor sections of the untreated animals. Interestingly, the tumor sections of the SQgem nanoassembly treated group showed a very low number of KI-67 positive proliferating cells, indicating a potent cell kill effect caused by SQgem nanoassemblies (Figure 6). The KI-67 index was calculated as 85, 55 and 11% for untreated, gemcitabine-treated and SQgem-treated tumors, respectively. On the other hand, the tumor sections treated with either the primary antibody alone or the secondary antibody alone did not show any brown staining, thus demonstrating KI-67 negative cell specific staining.

Discussion

The in vitro anticancer activity of SQgem nanoassemblies was measured on a panel of 60 human cancer cell lines under NCI drug screening program. On a wide variety of cell lines belonging to different categories of human cancers, the SQgem nanoassemblies showed potent in vitro cytotoxicity. Noteworthy, cell lines corresponding to non-small cell lung cancer, CNS cancer, melanoma and ovarian carcinoma were highly sensitive to the exposure of SQgem nanoassemblies. When compared with dose−response curves of gemcitabine (based on concentration required to reach 0% cell growth) on 60 human tumor cell panel available on the NCI Web site (NSC 613327, NCI Cancer Screen Current Data - DTP

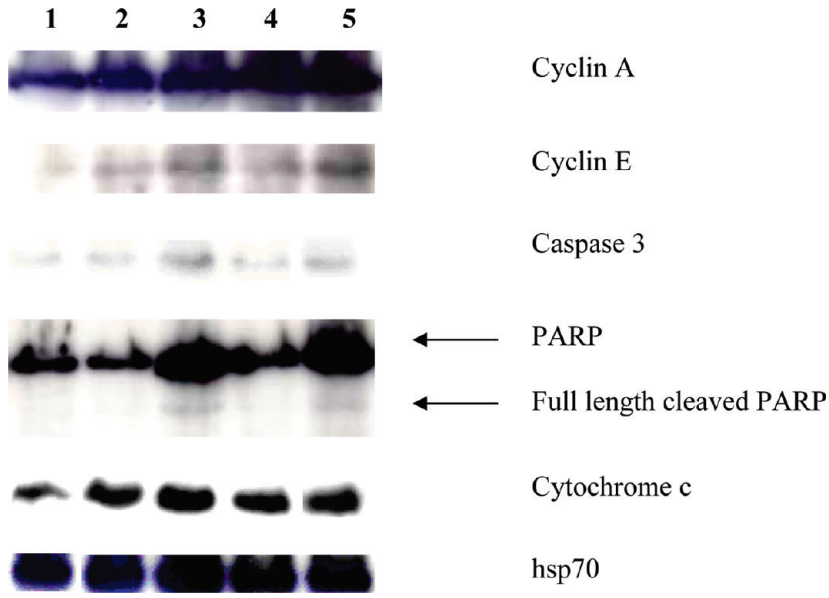

Figure 3. Cell cycle and apoptotic parameters using Western blot. L1210 wt cells (5×10^4) were incubated for 20 h with gemcitabine (10 and 20nM) and with SQgem nanoassemblies (SQgem NA) (10 and 20 nM equiv of gemcitabine) in RPMI 1640 supplemented with 10% fetal calf serum. Equal amounts of proteins (50 μg) were blotted with antibodies against cyclin A, cyclin E, activated caspase-3, PARP, cytochrome *c* according to Materials and Methods. The pattern shown is a representative of three different experiments. Hsp70 detection serves as constant protein loading for control. The order of the Western blots shown in the figure is as follows: (1) untreated cells, (2) gemcitabine 10 nM treated cells, (3) gemcitabine 20 nM treated cells, (4) SQgem nanoassemblies 10 nM equiv treated cells, and (5) SQgem nanoassembly 20 nM equiv treated cells.

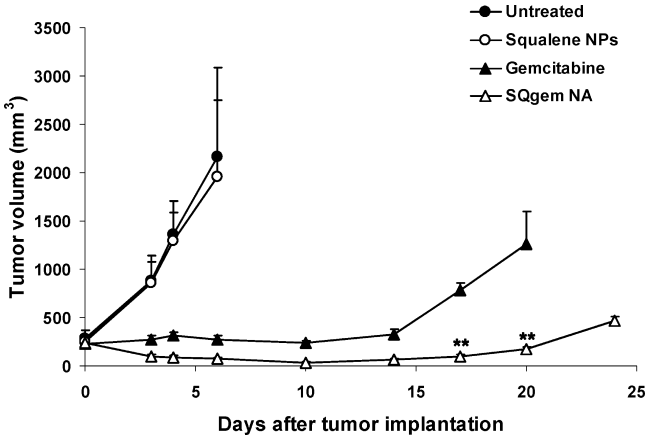

Figure 4. Antitumor activity of SQgem nanoassemblies (SQgem NA) (20 mg/kg equiv) compared with gemcitabine (100 mg/kg) against L1210 subcutaneous tumors in mice. The group of mice treated with squalene nanoparticles (100 mg/kg) was considered as a placebo. The values are the mean $\pm$ SD, $n = 6-7$. Statistical analysis was performed using Student's *t* test considering 95% confidence interval. The statistical test was very significant ** $p < 0.001$ compared with the gemcitabine-treated group.

60 cell/5 dose-05/2009), it has been found that the cytotoxicity of gemcitabine and SQgem nanoassemblies was similar against BT-459 breast cancer cell line, OVCAR-8 ovarian cancer cell line, SF-539 CNS cancer cell line, DU-145 prostate cancer cell line, and HOP-92 non-small cell lung cancer cell line. On the other hand, gemcitabine was more efficient compared with SQgem nanoassemblies, against HL-60 (TB) leukemia cells, OVCAR-5 ovarian cancer cells, NCI-H23 of non-small cell lung cancer cells, and SN12C and A498 renal cancer cells. On the contrary, SQgem nanoassemblies displayed more efficient cytotoxicity compared with gemcitabine against the majority of the remaining cell lines of different types such as breast, leukemia, ovarian, CNS, PC-3 prostate, colon, renal and non-small cell lung cancers. These results suggest the potential of this squalenoyl nanomedicine of gemcitabine for the treatment of human tumors. However, when tested on the L1210 wt murine cell line, the cytotoxicity of the SQgem nanoassemblies was lower than that exhibited by gemcitabine free. This was attributed to the prodrug nature of SQgem which needed to be activated by the intracellular lysosomal proteases cathepsins B and D before gemcitabine could be released to exert its anticancer activity. These lysosomal enzymes play a key role in degradation of amide-bearing drugs, in addition to some polypeptides and proteins within the cells. Moreover, cathepsin B was found overexpressed in tumors of cancer patients.[17−19] Thus, such cathepsin B overexpression is expected to facilitate better intracellular cleavage of SQgem, while SQgem remains adequately stable in plasma.[14] The important cytotoxicity of gemcitabine was further supported

(17) Kos, J.; Lah, L. Cysteine proteinases and their endogenous inhibitors: target proteins for prognosis, diagnosis and therapy in cancer. *Oncol. Rep.* **1998**, *5*, 1349–1361.

(18) Kos, J.; Sekirnik, A.; Premzl, A.; et al. Carboxypeptidases cathepsins X and B display distinct protein profile in human cells and tissues. *Exp. Cell Res.* **2005**, *306*, 103–113.

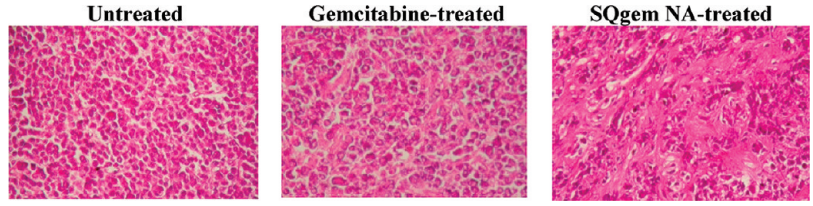

Figure 5. Histological examination of tumors obtained from mice, untreated or treated with either gemcitabine or SQgem nanoassemblies (SQgem NA). The tumors were embedded in paraffin and then processed for hematoxylin−eosin−saffran (HES) staining (magnification 40×). The images confirmed the higher population of cancer cells in the tumors of the gemcitabine-treated mice, as compared with the tumors of the SQgem nanoassembly treated mice.

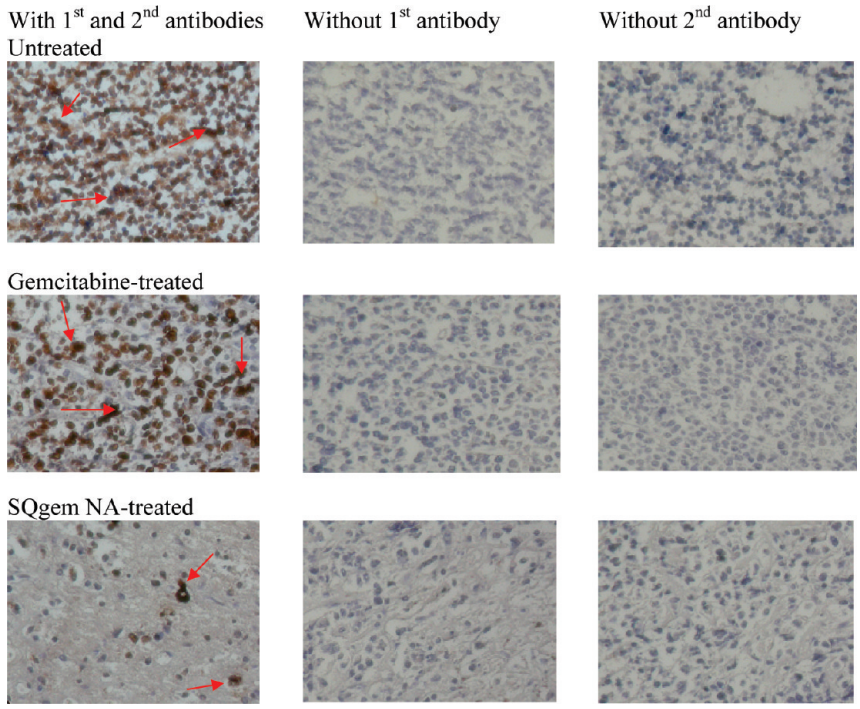

Figure 6. Immunochemical evaluation of tumors obtained from mice untreated or treated with either gemcitabine or SQgem nanoassemblies (SQgem NA). The tumors were paraffin embedded and then processed for cell proliferation test by staining the KI-67 antigen. Tumor sections were also treated either with first antibody alone or with second antibody alone (as false controls) to determine the nonspecific binding of the antibodies. The cells stained brown are KI-67 positive cells (indicated by arrows in the images). Noteworthy, tumor sections of the SQgem-treated mice showed considerably lower population of proliferating cells, comparatively to tumor sections of gemcitabine-treated mice.

by a considerably higher S-phase arrest and greater apoptosis induction in the gemcitabine-treated L1210 wt cells.

To highlight the mechanism of cytotoxicity of SQgem nanoassemblies on this cell line, Western blotting was performed on the SQgem treated cells. The protein expression profiling of the SQgem nanoassemblies-treated cells was characterized by an augmented expression of cyclins scanned such as cyclin A and cyclin E, the increase in cyclin E being much more pronounced than that of cyclin A. This is in agreement with a blockade of the cell cycle preferentially in G2/M phase.[20,21] Simultaneously, the activation of caspase-3 was noticed together with enhanced cleavage of PARP, suggesting the apoptosis induction.[22,23] Moreover, the increased cytochrome *c* level suggested the recruitment of a mitochondrial apoptotic triggered pathway,[24−26] but much more pronounced in the case of gemcitabine treatment than

(19) Premzl, A.; Zavasnik-Bergant, V.; Turk, V.; et al. Intracellular and extracellular cathepsin B facilitate invasion of MCF-10A neoT cells through reconstituted extracellular matrix in vitro. *Exp. Cell Res.* **2003**, *283*, 206–214.

(20) Coqueret, O. Linking cyclins to transcriptional control. *Genes* **2002**, *299*, 35–55.

(21) Scherr, C.; Roberts, J. M. Living with or without cyclins and cyclin-dependent kinases. *Genes Dev.* **2004**, *18*, 2699–2711.

(22) Kumar, S. Caspase function in programmed cell death. *Cell Death Differ.* **2007**, *14*, 32–43.

(23) Lamkanfi, M.; Festjens, N.; Declercq, W.; Vanden Berghe, T.; Vandenabeele, P. Caspase in cell survival, proliferation and differentiation. *Cell Death Differ.* **2007**, *14*, 44–55.

(24) Soldani, C.; Scovassi, A. I. Poly(ADP-ribose) polymerase-1 cleavage during apoptosis: an update. *Apoptosis* **2002**, *7*, 321–328.

(25) Oberst, A.; Bender, C.; Green, D. R. Living with death: the evolution of the mitochondrial pathway of apoptosis in animals. *Cell Death Differ.* **2008**, *15*, 1139–1146.

in SQgem nanoassembly treatment. However, from the above data, not much is known about any possible activity of SQgem affecting other apoptotic pathways. Moreover, it remains possible that gemcitabine is not solely affecting the cell survival by inducing apoptosis, because the cleavage of PARP may also reflect tissue necrosis.[27] Thus, the exact molecular mechanism of action of SQgem needs to be further elucidated.

The lower in vitro cytotoxicity of SQgem over gemcitabine and the differences in the above-discussed cell cycle events may be explained by the in vitro conditions: in SQgem nanoassemblies, the drug existed in the form of a reservoir whereas gemcitabine (when incubated free) was expected to quickly penetrate into the cancer cells, thus executing soon the anticancer activity, which was likely not the case with the SQgem prodrug. Alternatively, in the in vitro conditions wherein the tumor cells do not simulate the real tumors in terms of dense cell packing, gemcitabine released from SQgem following enzyme activity may likely diffuse into the culture medium, while in vivo inside the densely packed tumor, such diffusion would be into the neighboring tumor cells. Moreover, in vivo, the anticancer activity depends also on various other factors such as biological stability, pharmacokinetics, drug exposure pattern, drug penetration into tumor tissue and retention time in the cancer tissues etc. Thus, a drug with long biological half-life, improved biological stability and prolonged exposure could be expected to display an efficient anticancer activity in vivo. In this context, we recently observed that gemcitabine in the form of squalenoyl prodrug nanoassemblies displayed improved resistance to deamination in blood and also exhibited a greater plasmatic half-life and improved pharmacokinetics comparatively to free gemcitabine.[11] If SQgem nanoassemblies were found to be active in intravenously developed leukemia (due to preferential distribution and accumulation in spleen and liver),[12] their activity against solid tumors developed elsewhere in the body remained an open question since the additional barrier of the tumor vasculature need to be translocated. To answer, we developed here a subcutaneous solid tumor model using the same L1210 cell line in order to keep constant the sensitivity of the drug to the tumor cells, so that the activity depended principally on the tumor access of the drug. This model was also selected because tumor vascularization and microvessel density have been previously evidenced by immunohistochemistry.[28] Noteworthy, the subcutaneous implanted version of the L1210 leukemia has been already employed to study the tumor penetration of fluorescent latex particles to mimic liposomes[28] and to determine the antitumor activity of antisense oligonucleotide against the antiapoptotic Bcl2 loaded onto lipid nanoparticles.[29]

Interestingly, in this tumor model, the SQgem nanoassemblies displayed a superior anticancer activity over gemcitabine, clearly suggesting that SQgem was able to achieve sufficient solid tumor targeting to exhibit cancer cell kill, resulting in nodule regression. The superior anticancer activity of SQgem nanoassemblies over gemcitabine was further confirmed by histological observation of the treated tumors following HES staining. The data clearly indicated that the SQgem treatment wiped out a significant population of tumor cells from the cancer tissue, which was not the case following gemcitabine treatment.

However, it was not known whether the cells remaining in the tumor tissue (observed in histology studies) are proliferating or dead cells. Thus, to differentiate between the dead cell population with the proliferating cells remaining in the tumor tissue, KI-67 cell proliferation assay was performed by immunohistochemical staining of the tumor section. The Ki-67 protein is a cell proliferation antigen expressed in all phases of the cell cycle except G0 and serves as a good marker for proliferation.[30] Studies that have evaluated proliferation index by KI-67 immunohistochemistry, especially in breast cancer, have shown a significant correlation between high proliferation rates and shorter disease free and overall survival.[31,32] The lower KI-67 proliferation index in SQgem nanoassembly treated mice (11%) than in gemcitabine-treated mice (55%) clearly suggested the superiority of the SQgem nanoassembly treatment since only a very low number of proliferative cancer cells remained with this treatment.

Conclusion

This study demonstrates the high antiproliferative activity of the squalenoyl gemcitabine nanomedicine in a large panel of various cancer cells, suggesting its broad anticancer activity. The impressive anticancer effect observed against an aggressive and relatively resistant preclinical L1210 subcutaneously grafted tumor model argues for the superiority of this nanomedicine over its parent drug gemcitabine. Additionally, it has been confirmed that, mechanistically, the SQgem nanomedicine caused the tumor cell kill, at least in

(26) Chalah, A.; Khosravi-Far, R. The mitochondrial death pathway. *Adv. Exp. Med. Biol.* **2008**, *615*, 25–45.
(27) Kroemer, G.; Galluzzi, L.; Vandenabeele, P.; et al. Classification of cell death: recommendations of the nomenclature committee on cell death. *Cell Death Differ.* **2009**, *16*, 3–11.
(28) Pan, X.; Lee, R.; Ratnam, M. Penetration into solid tumor tissue of fluorescent latex microspheres: a mimic of liposome particles. *Anticancer Res.* **2004**, *24*, 3005–3008.
(29) Pan, X.; Chen, L.; Liu, S.; Gao, J.-X.; Lee, R. Antitumor activity of G3139 lipid nanoparticles (LNPs). *Mol. Pharmaceutics* **2009**, *6*, 211–220.
(30) Gerdes, J.; Lemke, H.; Baisch, H.; Wacker, H. H.; Schwab, U.; Stein, H. Cell cycle analysis of a cell proliferation-associated human nuclear antigen defined by the monoclonal antibody Ki-67. *J. Immunol.* **1984**, *133*, 1710–1715.
(31) Veronese, S. M.; Maisano, C.; Scibilia, J. Comparative prognostic value of Ki-67 and MIB-1 proliferation indices in breast cancer. *Anticancer Res.* **1995**, *15* (6B), 2717–2722.
(32) Liu, S.; Edgerton, S. M.; Moore, D. H., 2nd; Thor, A. D. Measures of cell turnover (proliferation and apoptosis) and their association with survival in breast cancer. *Clin. Cancer Res.* **2001**, *7*, 1716–1723.

part, through a mitochondrial apoptotic triggered pathway. Thus, this study makes obvious the potential of squalenoyl gemcitabine nanomedicine for the treatment of cancers, and recommends its candidature for clinical studies.

Acknowledgment. The financial support of the "Agence Nationale de la Recherche" (ANR, Grant SYLIANU) and of the CNRS (Grant "Ingénieur de valorisation") is acknowledged, as is a postdoctoral fellowship to L.H.R. from the Univ. Paris-Sud. The authors are grateful to National Cancer Institute, Frederick, MD, for selecting squalenoyl gemcitabine for in vitro screening studies. The authors are thankful to S. Mangenot for cryo-transmission electron microscopy.

MP900099E